PHYSICAL REVIEW B VOLUME 22, NUMBER 12 15 DECEMBER 1980

Electronic structure of magnetic impurities calculated from first principles

R. Podloucky,* R. Zeller, and P. H. Dederichs

Institut für Festkörperforschung der Kernforschungsanlage Jülich, D-5170 Jülich, Germany

(Received 2 June 1980)

The electronic structure of magnetic 3*d* impurities in Cu and Ag is calculated self-consistently from first principles. Using the density functional theory the exchange and correlation is treated in the local spin-density approximation of von Barth and Hedin. Our method is based on the Kohn-Korringa-Rostocker Green's-function method and the impurity is described by a single perturbed muffin-tin potential in an otherwise periodic lattice. We give results for the local density of states, the magnetic moments, and the phase shifts at the Fermi energy for the 3*d* impurities in Cu and Ag. Our results are in qualitative agreement with the Anderson model, however modifications due to the host band structure are important, especially for Mn and Fe in Cu. For all cases studied, the exchange integral I lies between 0.65 and 0.8 eV.

I. INTRODUCTION

Since the pioneering work of Anderson,[1] many experimental and theoretical efforts have been undertaken for the understanding of magnetic impurities in metals. Nevertheless, the nature of such impurities is not well understood. Two different theoretical models have been proposed: On the one hand, the Anderson model[1] or the equivalent Wolff model[2] which is based on Friedel's virtual bound-state concept, on the other hand the ionic model proposed by Schrieffer[3] and Hirst.[4] While both models have their proponents, the relevance of the models to the real systems in question is not clear.

In this paper we present *ab initio* calculations of the electronic structure of magnetic 3*d* impurities in Cu and Ag. We employ the density functional theory in the local spin-density approximation which has been proven to give very reliable results for ideal metals.[5] We use a Green's-function method, originally proposed by Dupree[6] and Beeby,[7] which is based on a muffin-tin approximation and the Korringa-Kohn-Rostoker (KKR)-band-structure method. In our model the impurity is described by a single perturbed muffin-tin potential in an otherwise periodic muffin-tin lattice. The Green's-function method has the major advantage that it correctly describes a single perturbation in an infinite crystal, i.e., the full spatial extent of the perturbed wave function is taken into account and only the perturbed potential is assumed to be localized. Other methods used in impurity calculations do not have this advantage. For instance, in cluster calculations one is always faced with problems due to the finite extent of the cluster, e.g., surface states, etc. Similarly, in supercell calculations, where a certain structure containing one defect is periodically repeated, one is plagued with uncontrollable interaction effects between the periodically arranged defects. The Green's function also allows us to make the calculation self-consistent with very little effort. First the ideal lattice Green's function is calculated from self-consistent host band structures. For the impurity calculation only the impurity muffin-tin potential has to be determined self-consistently, while during all iteration cycles the ideal lattice Green's function is unchanged. On the contrary, in cluster or supercell calculations all potentials have to be recalculated in each iteration cycle. In semiconductors a Green's-function method based on a linear combination of atomic orbitals (LCAO) expansion has successfully been applied recently for the calculation for the vacancy in silicon.[8, 9]

The organization of the paper is as follows: In Sec. II we give a short review of the KKR Green's-function method and discuss some problems arising in the application of this method. In Sec. III we discuss the results of our calculations for 3*d* impurities in Cu and Ag. In particular, we give results for the local densities of states, the magnetic moments, and the phase shifts at the Fermi energy. We also compare our results with recent cluster calculations of Johnson *et al.*[10] on the same systems. Both calculations do not agree and we think that the cluster calculations are unreliable. On the contrary, our results are in qualitative agreement with the phenomenological Anderson model. A preliminary account of this work has been published in Ref. 11.

II. KKR GREEN'S-FUNCTION METHOD

In the following we give a short review of the KKR Green's-function method for point-defect calculations. The results given here are not new and can be found in a number of articles, starting from the older work of Dupree,[6] Morgan,[12] and Beeby[7] to the more recent publications of Holzwarth,[13] Lehmann,[14] Harris,[15] and Hamasaki.[16] However, since this information is so widely scattered and since the nomenclature and the derivation of the most important formulas is always different, we think it is welcome and useful to give a short summary of the most important results.

A. Expansion into radial eigenfunctions

We consider the Green's function $G(\vec{r}, \vec{r}', E)$ for a periodic array of spherically symmetric muffin-tin potentials $v_m(|\vec{r}-\vec{R}^m|)$. For convenience we introduce new coordinates $\vec{R}^m+\vec{r}, \vec{R}^{m'}+\vec{r}'$ in each cell m and m' so that $\vec{r}$ and $\vec{r}'$ are always restricted to the Wigner-Seitz cell.

The Schrödinger equation of G in cell m is then:

$$\left(-\frac{\hbar^2}{2m}\,\partial^2_{\vec{r}}+v_m(r)-E\right)G(\vec{R}^m+\vec{r}, \vec{R}^{m'}+\vec{r}\,'; E)$$
$$=-\delta(\vec{r}-\vec{r}\,')\delta_{mm'}\,. \quad (1)$$

An analogous equation holds if $\vec{r}$ and $\vec{r}'$ are interchanged. For $m \neq m'$, G satisfies the homogeneous Schrödinger equation, since the source term vanishes. Therefore it can be expanded into radial eigenfunctions $R_l^m(r,E)Y_L(\vec{r})$. Here $Y_L(\vec{r})$ are real spherical harmonics and $R_l^m(r,E)$ are the regular solutions of the radial Schrödinger equation for the potential $v_m(r)$ and the energy E. Further, L stands for $L=(l,m)$. With this the Green's function can be written as

$$G(\vec{R}^m+\vec{r}, \vec{R}^{m'}+\vec{r}\,'; E)=\sum_{LL'} R_l^m(r,E)Y_L(\vec{r})G_{LL'}^{mm'}(E)R_{l'}^{m'}(r',E)Y_{L'}(\vec{r}\,')+\delta_{mm'}\frac{2m}{\hbar^2}K\sum_L R_l^m(r_<,E)Y_L(\vec{r})H_l^m(r_>,E)Y_L(\vec{r}\,')\,, \quad (2)$$

with

$$r_<=\min(r,r'),\quad r_>=\max(r,r'),\quad K=\left(\frac{2m}{\hbar^2}E\right)^{1/2}.$$

The coefficients $G_{LL'}^{mm'}(E)$ of the Green's functions have still to be determined (see below). For $m=m'$ the source term in (1) no longer vanishes and we have to add the second term in Eq. (2), which represents the Green's function G_S^m for a single muffin-tin potential $v_m(r)$ embedded in free space. The construction of this Green's function is quite analogous to the radial expansion of the potential free Green's function. The regular solution $R_l^m(r,E)$ corresponds to the spherical Bessel function; H_l^m corresponds to the spherical Hankel function and contains both the nonregular solution $N_l^m(r,E)$ and the regular solution $R_l^m(r,E)$:

$$H_l^m(r,E)=N_l^m(r,E)-iR_l^m(r,E)\,. \quad (3)$$

Both the regular and the nonregular solution can be chosen as real and outside the muffin-tin radius R_{MT} they are given in terms of the spherical Bessel function $j_l(Kr)$ and the spherical Neumann function $n_l(Kr)$.

$$\left.\begin{aligned}R_l^m(r,E)&=\cos\delta_l^m(E)j_l(Kr)-\sin\delta_l^m(E)n_l(Kr)\,,\\ N_l^m(r,E)&=+\sin\delta_l^m(E)j_l(Kr)+\cos\delta_l^m(E)n_l(Kr)\,.\end{aligned}\right\} r\geq R_{\mathrm{MT}} \quad (4)$$

It is clear from the construction of expression (2), that the Green's function satisfies in each cell the Schrödinger equation (1). The connection between the different cells can be made by determining the elements $G_{LL'}^{mm'}(E)$.

B. Matrix elements $G_{LL'}^{mm'}$ of the defect Green's function

For practical applications it is very useful to have a connection between the Green's function G for an arbitrary defect structure, i.e., arbitrary potentials $v_m(r)$, and the ideal host Green's function G^0 for a given host potential $v^0(r)$ in each cell, as well as the free-space Green's function g for vanishing potentials. For all three cases Eq. (2) remains valid if one replaces R_l^m and N_l^m by the host radial functions $R_l^0(r,E)$ and $N_l^0(r,E)$, respectively, the spherical Bessel and Neumann functions $j_l(Kr)$ and $n_l(Kr)$. The corresponding elements we call $G_{LL'}^{0\,(m-m')}(E)$ for the host-lattice case and $g_{LL'}^{(m-m')}(E)$ for the free space. A simple algebraic equation between these elements is obtained by inserting the corresponding expressions (2) for the Green's functions in the following Lippmann-Schwinger equations for G:

$$G(\vec{R}^m+\vec{r}, \vec{R}^{m'}+\vec{r}\,')=g(\vec{R}^m+\vec{r}, \vec{R}^{m'}+\vec{r}\,')+\sum_n\int d\vec{r}\,''g(\vec{R}^m+\vec{r}, \vec{R}^n+\vec{r}\,'')v_n(r'')G(\vec{R}^n+\vec{r}\,'', \vec{R}^{m'}+\vec{r}\,')\,, \quad (5)$$

$$G(\vec{R}^m+\vec{r}, \vec{R}^{m'}+\vec{r}\,')=G^0(\vec{R}^m+\vec{r}, \vec{R}^{m'}+\vec{r}\,')+\sum_n\int d\vec{r}\,''G^0(\vec{R}^m+\vec{r}, \vec{R}^n+\vec{r}\,'')\Delta v_n(r'')G(\vec{R}^n+\vec{r}\,'', \vec{R}^{m'}+\vec{r}\,')\,, \quad (6)$$

with $\Delta v_n(r) = v_n(r) - v^0(r)$. A straightforward calculation (see the Appendix) yields

$$\tilde{G}^{mm'}_{LL'}(E) = g^{(m-m')}_{LL'}(E) + \sum_{n,L''} g^{(m-n)}_{LL''} t^n_{l''}(E) \tilde{G}^{nm'}_{L''L'}(E) \tag{7}$$

when the free-space Green's function is taken as reference or

$$\tilde{G}^{mm'}_{LL'}(E) = \tilde{G}^{0(m-m')}_{LL'}(E) + \sum_{n,L''} \tilde{G}^{0(m-n)}_{LL'}(E) \Delta t^n_{l''}(E) \tilde{G}^{nm'}_{L''L'}(E) , \tag{8}$$

with

$$\tilde{G}^{mm'}_{LL'} = e^{-i\delta^m_l} G^{mm'}_{LL'} e^{-i\delta^{m'}_{l'}} , \quad \tilde{G}^{0mm'}_{LL} = e^{-i\delta^0_l} G^{0mm'}_{LL'} e^{-i\delta^0_l} , \tag{9}$$

when the host Green's function G^0 is taken as reference. Instead of the potentials we have in these equations the "on-shell" t matrices as perturbation:

$$\begin{aligned} t^m_l(E) &= -\frac{\hbar^2}{2m} \frac{1}{K} e^{i\delta^m_l(E)} \sin\delta^m_l(E), \\ \Delta t^m_l(E) &= t^m_l(E) - t^0_l(E) . \end{aligned} \tag{10}$$

Whereas in cluster calculations, i.e., for the scattering at a finite number of particles, the free-space equations (7) are most appropriate, for the description of a defect in an infinite crystal clearly the equations (8) are to be preferred, since the perturbation Δt^n_l is then restricted to the immediate vicinity of the defect. On the right-hand side of Eq. (8) only those Green's functions in the perturbed subspace near the defect enter. For example, if n potentials are perturbed and if on each site $l_{\max}$ perturbed phase shifts have to be taken into account, then Eq. (8) requires the inversion of matrices of dimension $n(l_{\max}+1)^2$. Thus Eq. (8) is not more difficult to solve than Eq. (7) for a cluster in free space, provided the disturbance is of similar size and the host Green's functions $G^{0(m-n)}_{LL'}(E)$ are known.

Equation (8) strongly simplifies, if only the impurity potential at site $n=0$ is perturbed, since then only $\Delta t^{n=0}_l$ enters. Of primary interest is the impurity Green's function $G^{m=0\ m'=0}_{LL'}(E)$. For cubic symmetry and for $l_{\max} \leqslant 2$, this Green's function is diagonal, $\tilde{G}^{00}_{LL'}(E) = \tilde{G}_{(L)} \delta_{LL'}$ and the solution of Eq. (8) trivially becomes

$$\tilde{G}_{(L)} = \frac{1}{1 - \tilde{G}^0_{(L)} \Delta t_l} \tilde{G}^0_{(L)} . \tag{11}$$

Throughout the paper we will restrict our discussion to this model, where only the impurity potential itself is disturbed, essentially assuming that the impurity is fully screened within its own muffin tin.

C. Evaluation of the host Green's function

The major prolbem of the KKR Green's-function method is the determination of the ideal-lattice Green's function G^0. Starting with the spectral representation (BZ denotes Brillouin zone)

$$G(\vec{R}^m + \vec{r}, \vec{R}^{m'} + \vec{r}'; E) = \sum_\nu \int_{\mathrm{BZ}} d\mathrm{k} \frac{\psi^0_{\vec{k}\nu}(\vec{R}^m + \vec{r}) \psi^{0*}_{\vec{k}\nu}(\vec{R}^{m'} + \vec{r}')}{E + i0^+ - E_{\vec{k}\nu}} , \tag{12}$$

we may insert the usual KKR ansatz for the wave functions:

$$\psi^0_{\vec{k}\nu}(\vec{R}^m + \vec{r}) = e^{i\vec{k}\cdot\vec{R}^m} \sum_L i^l \phi_L(\vec{k}\nu) R^0_l(r, E) Y_L(\vec{r}) . \tag{13}$$

By comparing with the general result (2) for G^0 we obtain for the imaginary part of $G^{0\,(m-m')}_{LL'}$

$$\mathrm{Im} G^{0\,(m-m')}_{LL'}(E) = \frac{2m}{\hbar^2} K \Theta(E) \delta_{mm'} \delta_{LL'} - \pi \sum_\nu \int_{\mathrm{BZ}} d\vec{k}\, \delta(E - E_{\vec{k}\nu}) \phi_L(\vec{k}\nu) \phi^*_{L'}(\vec{k}\nu) i^{l-l'} e^{i\vec{k}\cdot(\vec{R}^m - \vec{R}^{m'})} . \tag{14}$$

In this form the imaginary part can be directly evaluated by a numerical Brillouin-zone integration. The real part can be obtained from the imaginary one by a Kramers-Kronig integration. In Eq. (2) we note that both $G(\vec{R}^m + \vec{r}, \vec{R}^{m'} + \vec{r}')$ as well as the term proportional to $\delta_{mm'}$, representing the Green's function for a single muffin-tin potential, obey a Kramers-Kronig relation, since they are both proper Green's functions. Therefore, also the third term containing the elements $G^{mm'}_{LL'}(E)$ fulfills a Kramers-Kronig relation. Thus we obtain

$$\alpha_{ll'}(E)\, \mathrm{Re} G^{0\,(m-m')}_{LL'}(E) = \frac{1}{\pi} \int_{-\infty}^{+\infty} dE' P\left(\frac{1}{E - E'}\right) \alpha_{ll'}(E')\, \mathrm{Im} G^{0\,(m-m')}_{LL'}(E') \tag{15}$$

with

$$\alpha_{ll'}(E) = \int_0^{R_{\mathrm{MT}}} r^2 dr\, R^0_l(r, E) R^0_{l'}(r, E) ,$$

where, for convenience, we have integrated out the radial dependence.

In actual calculations the E' integration in (15) requires the knowledge of the band structure up to infinite energies. Since this is impossible, one has to choose a cutoff energy E_c. For $m=m'$ this means that above E_c one replaces the Green's function by that for free electrons [compare Eq. (14)].

Alternatively one can calculate the Green's-function elements $G^{0\,(m-m')}_{LL'}(E)$ from the free-electron Green's function $g^{m-m'}_{LL'}(E)$. Analogously to Eq. (7) we obtain

$$\tilde{G}^{0\,(m-m')}_{LL'}(E)=g^{(m-m')}_{LL'}(E)+\sum_{n,L''}g^{(m-n)}_{LL''}(E)t^{0}_{l''}(E)\tilde{G}^{0\,(n-m')}_{L''L'}(E)\,. \tag{16}$$

Owing to translation invariance this equation can be solved by Fourier transformation leading to

$$\tilde{G}^{0\,(m-m')}_{LL'}(E)=\frac{1}{V_{\mathrm{BZ}}}\int_{\mathrm{BZ}}d\vec{\mathrm{k}}\sum_{L''}\left(\frac{1}{1-g(\vec{\mathrm{k}}E)t(E)}\right)_{LL''}g_{L''L'}(\vec{\mathrm{k}}E)e^{i\vec{\mathrm{k}}\cdot(\vec{\mathrm{R}}^m-\vec{\mathrm{R}}^{m'})}$$

with

$$g_{LL'}(\vec{\mathrm{k}}E)=\sum_m e^{i\vec{\mathrm{k}}\cdot(\vec{\mathrm{R}}^m-\vec{\mathrm{R}}^{m'})}g^{(m-m')}_{LL'}(E)\,. \tag{17}$$

The $g_{LL'}(\vec{\mathrm{k}}E)$ are directly related to the KKR structure constants. Contrary to (15), the integrand (17) is only needed in the desired energy range. However, here additional difficulties arise due to the strong E and $\vec{\mathrm{k}}$ dependence of the KKR structure constants, which requires a very good numerical Brillouin-zone integration. Detailed calculations with both methods[17] show that the much faster Kramers-Kronig calculation with a cutoff at about 1 Ry can be used without significant errors. The BZ integrations are performed by the tetrahedron method[17] with 6144 tetrahedrons in the irreducible part of the Brillouin zone.

D. Charge densities and local densities of states

The imaginary part of the Green's function gives the distribution $n(\vec{\mathrm{r}},E)$ of electrons in space and energy:

$$n(\vec{\mathrm{r}},E)=-\frac{2}{\pi}\,\mathrm{Im}G(\vec{\mathrm{r}},\vec{\mathrm{r}};E)\,. \tag{18}$$

From this the charge density is calculated by energy integration,

$$n(\vec{\mathrm{r}})=\int_{-\infty}^{E_F}dE\,\frac{-2}{\pi}\,\mathrm{Im}G(\vec{\mathrm{r}},\vec{\mathrm{r}};E)\,, \tag{19}$$

whereas the local density of states, e.g., in the impurity cell V_I, follows as

$$n_{\mathrm{loc}}(E)=\int_{V_I}d\vec{\mathrm{r}}\,\frac{-2}{\pi}\,\mathrm{Im}G(\vec{\mathrm{r}},\vec{\mathrm{r}};E)\,. \tag{20}$$

The total charge in the impurity cell is then

$$N_{\mathrm{loc}}=\int_{-\infty}^{E_F}dE\,n_{\mathrm{loc}}(E)=\int_{V_I}d\vec{\mathrm{r}}\,n(\vec{\mathrm{r}})\,. \tag{21}$$

Contrary to these local properties one can also calculate the change of the total density of states due to the impurity, where also effects due to the polarization of neighboring host atoms are included. According to Lloyd's formula,[18] the change of the integrated density of states due to the impurity is for our model with one perturbed muffin tin given by

$$\begin{aligned}\Delta N(E)&=\frac{2}{\pi}\sum_L\{(\delta_l-\delta^0_l)-\mathrm{Im}\ln[1-\tilde{G}^0_{(L)}(E)\Delta t_l(E)]\}\\&=\frac{2}{\pi}\sum_L(\Delta\delta_l+\phi_L)=\frac{2}{\pi}\sum_L\eta_L(E)\,,\end{aligned} \tag{22}$$

where we have set

$$A_L(E)=[1-\tilde{G}^0_{(L)}(E)\Delta t_l(E)]^{-1}=|A_L|e^{i\phi_L}\,.$$

The phase shifts $\eta_L=\Delta\delta_l+\phi_L$ are called generalized Friedel phase shifts and consist of the usual contribution $\Delta\delta_l$ due to the changed impurity phase shifts and an additional contribution ϕ_L, arising from an interference of the impurity scattering with intermediate "backscattering" events at the host atoms. According to Friedel's sum rule, a completely self-consistent calculation should give $\Delta N(E_F)=\Delta Z$, the changed nuclear charge of the impurity, since the impurity would be totally screened in a metal.

E. Inclusion of spin polarization

In the case of spin polarization we have two different potentials $v^m_\pm(r)$, for up spin (v_+) and down spin (v_-). Consequently all phase shifts, Green's functions, etc., obtain an additional index + or − for the spin, e.g., $\delta^m_{\pm\,l}(E)$, $G^{mm'}_{\pm\,LL'}(E)$, and all equations in Secs. II A–II C appear twofold, one for each spin direction.

The densities of electrons with spin up (+) or down (−) are given by

$$\begin{aligned}n_\pm(\vec{\mathrm{r}})&=\int_{-\infty}^{E_F}dE\,\frac{-1}{\pi}\,\mathrm{Im}G_\pm(\vec{\mathrm{r}},\vec{\mathrm{r}};E)\,,\\n^\pm_{\mathrm{loc}}(E)&=\int_{V_I}d\vec{\mathrm{r}}\,\frac{-1}{\pi}\,\mathrm{Im}G_\pm(\vec{\mathrm{r}},\vec{\mathrm{r}},E)\,.\end{aligned} \tag{23}$$

The local charge N_{loc} and the local moment M_{loc}

within the impurity cell are then

$$M_{\mathrm{loc}}=N^{+}_{\mathrm{loc}}-N^{+}_{\mathrm{loc}}$$

$$=\int_{-\infty}^{E_F} dE[n^{+}_{\mathrm{loc}}(E)-n^{-}_{\mathrm{loc}}(E)]=\int_{V_I} d\vec{\mathrm{r}}[n^{+}(\vec{\mathrm{r}})-n^{-}(\vec{\mathrm{r}})], \tag{24}$$

$$N_{\mathrm{loc}}=N^{+}_{\mathrm{loc}}+N^{-}_{\mathrm{loc}}.$$

From Lloyd's formula one obtains for the total displaced charge due to the impurity

$$\Delta N(E_F)=\Delta N^{+}(E_F)+\Delta N^{-}(E_F), \tag{25}$$

whereas the change of the magnetic moment is

$$\Delta M=\Delta N^{+}(E_F)-\Delta N^{-}(E_F)=M_{\mathrm{tot}}. \tag{26}$$

For a nonmagnetic host this is just the total moment M_{tot} due to the impurity where contributions due to the polarization of neighboring host atoms are included, which is not the case for M_{loc}.

F. Density functional theory and self-consistency

For our calculations we have applied the density functional formalism. Exchange and correlation are treated in the local spin-density approximation suggested by von Barth and Hedin[19]:

$$V_{\mathrm{xc}}=-1.221774/r_s(1\pm\zeta)^{1/3}-C_p\ln(1+r_p/r_s)$$
$$+5.1298[C_F F(r_F/r_s)-C_p F(r_p/r_s)]$$
$$\times[1-(1\pm\zeta)^{1/3}], \tag{27}$$

where

$$F(z)=(1+z^3)\ln\left(1+\frac{1}{z}\right)+\frac{z}{2}-z^2-\frac{1}{3},$$

$$r_s=\left(\frac{3}{4\pi n}\right)^{1/3}, \quad \zeta=\frac{n^{+}-n^{-}}{n}.$$

The parameters $C_p=0.045$, $C_F=C_{p/2}$, $r_p=21$, $r_F=2^{4/3}r_p$ were chosen to agree with those of Moruzzi *et al.*[20]

The host band structures of Cu and Ag were generated from the self-consistent potentials given by Moruzzi *et al.*[20] The ideal Green's functions are then calculated by a Brillouin-zone integration. These two time-consuming steps of the calculations have to be performed only once for each host metal. This represents a major advantage of a Green's-function method since the subsequent calculations for the defect Green's function [Eqs. (11) and (2)] and the impurity charge densities [Eq. (19)] are rather fast. Only these fast steps have to be repeated for each impurity, and that many times since the self-consistent solution for the impurity potential is obtained as usual by an iteration technique.

Several problems are connected with the iteration procedure: An initial guess for the impurity potential has to be found, the charge density has to be calculated everywhere for solving Poisson's equation for the potential, the straightforward iteration procedure is usually unstable, and the magnetic moment converges rather slowly.

As input to the first iteration step we used either a potential constructed by a Mattheiss prescription from Herman-Skillman atomic charge densities or an already self-consistently determined impurity potential of an element adjacent in the Periodic Table. When solving Poisson's equation we confine the perturbation in charge density to the impurity muffin tin. This approximation changes the impurity potential by a constant equal for both spins and is one of the reasons why the Friedel sum rule is not completely fulfilled (see Table IV). For convenience the impurity core states are treated as frozen and the core charge density was taken from an atomic calculation.

As in atomic or band-structure calculations the straightforward iteration which uses the output potential of one iteration as the input to the next iteration does not converge due to the strong Coulomb forces. In defect calculations a similar effect also arises since the Fermi energy E_F is fixed by the host and therefore the number of electrons is not conserved. A small shift of the potential leads to a small energy shift of a virtual bound state, but to a large change of the charge in the impurity cell, particularly if the virtual bound state lies near E_F. For stabilizing the iteration process we adopted the standard procedure of using a linear combination of input and output potentials from one iteration as input potential for the next iteration. However the mixing factor, the amount of output potential used, is rather small, typically a few percent, which leads to a hundred or more iterations. For accelerating the convergence of the magnetic moments we used a larger mixing factor acting only on the difference between the potentials for up and down spin. The iteration process is stopped if input and output potentials of one iteration agree on the average to better than 0.01 eV. The final results for impurity potentials do not depend on the initial guess of the potentials and on the applied mixing factors.

III. RESULTS AND DISCUSSION

A. Local density of states

The local densities of states (20) in the impurity Wigner-Seitz cell are plotted in Figs 1(b)–1(h) for the 3*d* impurities Ti–Ni in Ag, both for the majority and the minority spin. For comparison Fig. 1(a) gives the density of states of pure Ag.

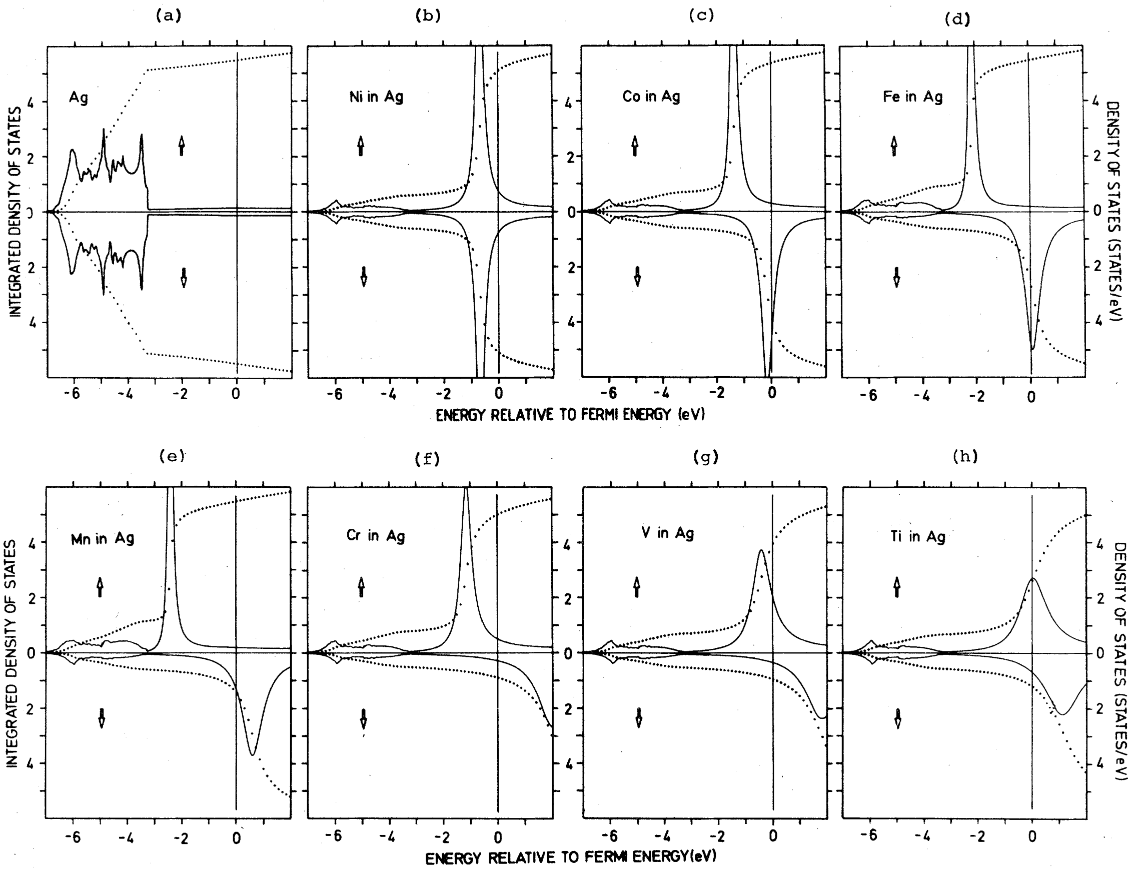

FIG. 1. Local density of states (full lines) and integrated local density of states (dotted lines) for majority (↑) and minority (↓) spin of 3d impurities in Ag. For comparison (a) gives the density of states of pure Ag.

Since Ag is nonmagnetic, the densities for both spin directions agree. The dotted lines give the integrated local densities of state. Their difference represents the number of unpaired electrons with energy smaller than E and thus at the Fermi energy the local moment in the impurity cell [see Eq. (24)]. All 3d impurities show Lorentzian-shaped virtual bound states near the Fermi energy. In Ag, only Ni is nonmagnetic; all others show a considerable spin splitting and thus a local moment, which is especially large for Fe, Mn, and Cr. This behavior is just as expected from the Anderson model. Band-structure effects from the silver d band are not very important.

This situation is different for 3d impurities in Cu. Figures 2(a) and 2(b) show the local densities of states for Cr and Mn in Cu. Contrary to Ag, the d band of Cu is higher in energy, extending between 1.6 and 5.3 eV below E_F. For Cr one still has a split Lorentzian; the majority peak of Mn [and also of Fe (Ref. 11)] is extremely narrow and contains only about two electrons, whereas more intensity (2.5 electrons) is distributed in the range of the Cu d band. The latter behavior can also be seen already for Cr in Cu. It arises from a local hybridization between the impurity d orbitals with the d orbitals of the neighboring host atoms and cannot be described by the Anderson model or other models which neglected the host band structure, e.g., an impurity-in-jellium model.[21] Figures 2(c) and 2(d) show the results of such a calculation, where only the scattering at the impurity muffin-tin is taken into account, and the scattering at the host muffin-tin is neglected. Technically this is obtained from expression (2) for the impurity Green's function if the elements $G_{LL'}^{mm'}$ are set equal to zero. (These jellium calculations are not self-consistent; rather, we have taken the impurity potential from the full Cr-in-Cu and Mn-in-Cu calculation.)

The peak positions and the half-widths of the virtual bound states for both spin directions are given in Table I for all 3d impurities in Cu and Ag. In principle each virtual bound d state consists of two separate peaks for the d-t_{2g} and d-e_g symmetries, which are split due to the crystal field. In practice this crystal-field splitting is much smaller than the half-widths of the peaks

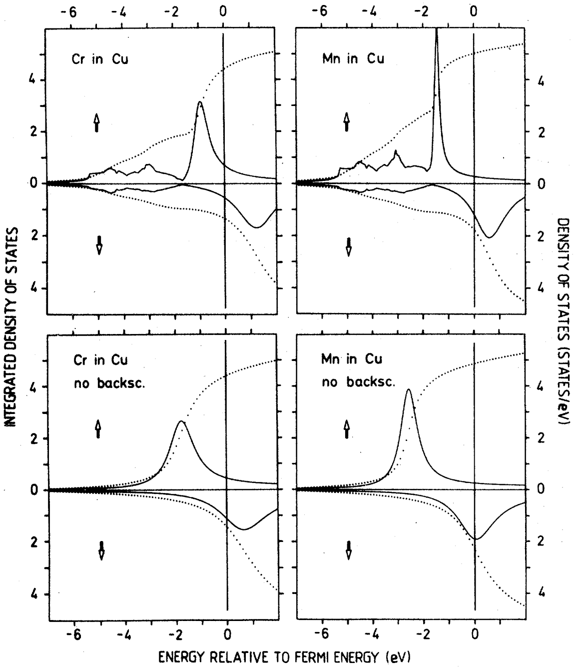

FIG. 2. Local density of states (full lines) and integrated local density of states (dotted lines) for Cr in Cu (a) and Mn in Cu (b). (c) and (d) give the same quantities in the approximation that backscattering effects are neglected (jellium model).

and therefore quite unimportant. As is also seen from Fig. 1, the majority peak moves in the sequence Ti to Ni from above the Fermi energy to below the Fermi energy with a minimum at Mn (− 1.44 eV in Cu and − 2.42 eV in Ag). The spin splitting of the peaks is largest in the middle of this series (2.17 eV for Cr in Cu and 3.20 eV for Cr in Ag) and considerable larger in Ag than in Cu (see the discussion below).

The half-widths of the virtual bound states are in general much smaller than the ones obtained in a jellium model (see Fig. 2). Especially the small values of the majority peaks for Mn and Fe in Cu, and to smaller extent also in Ag, are effects of the host band structure. In general, the half-widths in Ag are smaller than the ones in Cu.

In the Anderson model, the half-width Γ is proportional to the host density of states at the Fermi energy times the square of the s-d matrix element V_{sd}:

$$\Gamma = 2\pi |V_{sd}|^2 n(E_F) . \tag{28}$$

From the jellium calculations we obtain that Γ is roughly a factor 1.6 larger for impurities in Cu jellium than in Ag jellium. A change by about 15% can be explained by the larger s density of Cu, resulting from a 15% smaller lattice constant. This would mean, that the matrix element V_{sd} would be somewhat larger in Ag than in Cu (about 20%).

Photoemission measurements of Norris and Walldén[22] and Walldén[23] at dilute *Ag*Mn show a broad hump in the photoemitted intensity between 1.8 and 3.2 eV which compares favorably with our peak maximum of the majority spin at 2.42 eV. On the contrary, for *Cu*Mn no indication of a virtual bound state peak has been found. An explanation for this negative result could be the strong overlap of the Mn density of state with the one of pure Cu, as is shown in Fig. 2(b). Optical-data measurements of Myers *et al.*[24] and Steel and Treherne[25] lead to similar findings, two rather broad impurity peaks for *Ag*Mn, presumably one due to the majority and the other due to the minority spin states, but no indication of additional impurity peaks for *Cu*Mn.

Recently extensive x-ray photoemission spectroscopy (XPS) studies of 3d impurities in noble metals have been performed by Höchst, Steiner, and Hüfner.[26] In these measurements clearly defined virtual bound states are only detected for *Cu*Ni and *Au*Ni, however, not for magnetic impurities such as *Ag*Mn, *Au*Fe, or *Cu*Fe. Here only an increase in the region of the flat s-p band between the host d band and the Fermi energy is found. Also a considerable increase within the range of the host d band is reported. Part of the experimental results are explained by the recent cluster calculations of Johnson *et al.*,[10] which we, however, consider as unreliable (see the discus-

TABLE I. Peak positions [column (a)] and half-widths [column (b)] of the virtual bound states of 3d impurities in Cu and Ag for both spin directions. All values are in eV.

							Impurity								
		Ti		V		Cr		Mn		Fe		Co		Ni	
Host	Spin	(a)	(b)	(a)	(b)	(a)	(b)	(a)	(b)	(a)	(b)	(a)	(b)	(a)	(b)
Cu	↑	0.62	2.04	−0.21	1.39	−0.91	0.69	−1.44	0.24	−1.44	0.23	−0.70	0.64	−1.09	0.38
	↓	0.62	2.04	0.85	1.87	1.26	1.70	0.62	1.47	0.03	1.09	−0.70	0.64	−1.09	0.38
Ag	↑	0.05	1.21	−0.41	0.84	−1.15	0.48	−2.42	0.18	−2.14	0.18	−1.38	0.27	−0.69	0.33
	↓	1.13	1.59	1.83	1.46	2.05	1.25	0.60	0.91	0.07	0.66	−0.16	0.51	−0.69	0.33

sion in Sec. IIIC). While these new results cast some doubts on the earlier photoemission measurements,[22,23] they are also in conflict with our well-defined virtual bound states shown in Figs. 1 and 2. The reason for this discrepancy is not clear to us. In this respect it is worthwhile to mention that within the density functional theory the energy eigenvalues and thus the densities of states do not have a direct physical meaning. Thus we cannot exclude that, while our results for the charge and magnetization density would be perfectly sound, the densities of states could be strongly modified by many-body effects (See Note added).

Coleridge *et al.*[27] have performed de Haas-van Alphen (dHvA) measurements at very diluted *Cu*Cr, *Cu*Mn, and *Cu*Fe. For *Cu*Cr their results show that the virtual bound states of Cr scatter electrons of both spins equally well, in good agreement with the symmetric location of the virtual bound states of Cr in Fig. 2(a). For *Cu*Mn the scattering is asymmetric for the two conduction-electron-spin states, whereas for *Cu*Fe resonance scattering at the minority virtual bound states occurs,[28] both in agreement with our calculations (see Fig. 2 and Table I).

B. Magnetic moments

Figures 3(a) and 3(b) show the local moment in the Wigner-Seitz cell of the impurity [open circles, see Eq. (24)] and the total moment which includes the polarization of the host atoms [full circles, see Eq. (26)]. The moments are given in units of unpaired electrons, corresponding to one Bohr magneton (for a g value of $g=2$). The triangles give experimental values for the moments as obtained by susceptibility measurements or neutron scattering. Not included in the figure is a recent experimental value of 4.6 for Cr in Ag.[29]

Our self-consistent calculations show Ti, Co, and Ni to be nonmagnetic in Cu, whereas in Ag only Ni is nonmagnetic. In general there is a stronger tendency for magnetism in Ag than in Cu, which is also seen from the larger moments. This is in line with the larger spin splitting between the peaks of the majority and minority virtual bound states, which is also plotted in Fig. 3 (crosses connected by full lines). According to the Anderson model[1] or the Stoner model, the splitting $\Delta E_d = IM_{\text{loc}}$ is proportional to the local magnetic moment, where I is the exchange inte-

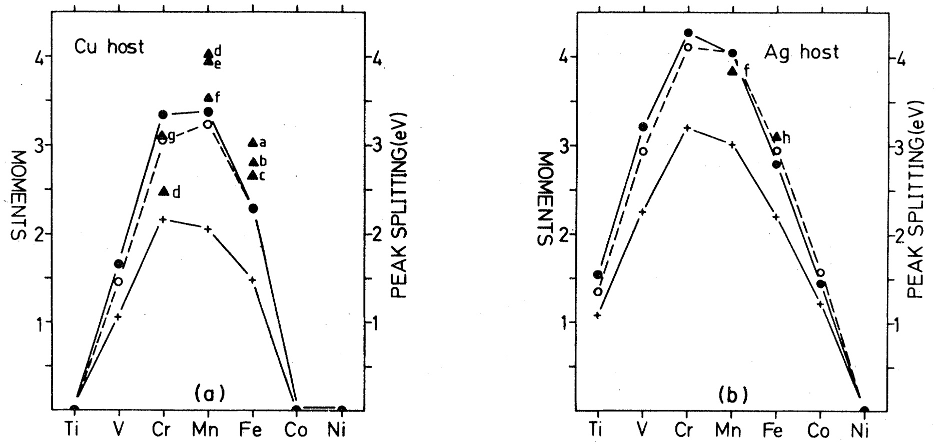

FIG. 3. Local moments (open circles connected by dashed line) and total moments (full circles connected by full line) of $3d$ impurities in Cu and Ag. The triangles are experimental results of different authors. The moments are given in units of Bohr magnetons. Also included in (a) and (b) is the exchange splitting of the virtual bound states (crosses connected by full lines) showing the proportionality of the peak splitting with the local moments. Data points refer to the following:

[a] J. R. Davis and T. J. Hicks, J. Phys. F 9, L7 (1979).
[b] C. M. Hurd, J. Phys. Chem. Solids 28, 1345 (1967).
[c] P. Steiner, S. Hüfner, and W. V. Zdrojewsky, Phys. Rev. B 10, 4704 (1974).
[d] W. D. Weiss, Z. Mettallk. 58, 909 (1967).
[e] J. R. Davis and T. J. Hicks, J. Phys. F 9, 753 (1979).
[f] C. M. Hurd, J. Phys. Chem. Solids 30, 539 (1969).
[g] M. Vochten, M. Labro, and S. Vynckier, Physica 86–88B, 467 (1977).
[h] P. Steiner and S. Hüfner, Phys. Rev. B 12, 842 (1975).

gral. This proportionality can be directly seen from Figs. 3(a) and 3(b) (compare the peak splitting with the moment). In Ag we obtain for I values between 0.74 and 0.80 eV, whereas in Cu we have 0.74 eV for V, 0.74 eV for Cr, and 0.64 eV both for Mn and Fe. The smaller value for Mn and Fe in Cu is due to the fact that the position of the sharp majority peak is no longer characteristic for the energy distribution of most majority electrons [see Fig. 2(b)]. The values for I obtained here are slightly smaller than theoretical estimates by Moruzzi *et al.*[22] and Gunnarson[30] for the exchange integral in pure crystal, whereas recent experimental conclusions of Eastman *et al.*[5] lead to a value of 0.6 to 0.7 eV for pure Fe, Co, and Ni metals. Our result is that the magnetism is more favored in Ag than in Cu, can also be explained by the Anderson model: Favorable conditions are a small host density of states, a small s-d coupling V_{sd}, but a large exchange integral I. All these conditions slightly favor Ag over Cu (see also the discussion of the halfwidths of the virtual bound states in the preceding section).

The comparison of the calculated moments with the experimental values is satisfactory. Apparently the experimental values do scatter appreciably. Moreover, one should realize that results of susceptibility measurements or neutron scattering cannot be interpreted in a straightforward fashion in an itinerant theory.

Figures 3(a) and 3(b) show that the local and the total moments of the impurity agree quite well, which means that the polarization of the neighboring host atoms is not very important. This is an *a posteriori* justification of our model assumption that the perturbed potential, and thus also its exchange correlation part, has been restricted to the impurity muffin tin. Nevertheless, the small but systematic difference between the local and the total moments is quite interesting: it even changes sign. For instance in Ag, the host atoms enhance the moments of the impurities Ti, V, and Cr, whereas they diminish the moments of Fe and Co. Both for Cu and Ag, most of the host polarization comes from the host d electrons, and not from the s electrons as assumed in the Anderson model.

C. Phase shifts at the Fermi

In Table II we have summarized the generalized Friedel phase shifts $\eta_L(E_F)$ of Eq. (22). For each spin direction we have an s, p, t_{2g}, and e_g phase shift ($\eta_s, \eta_p, \eta_{t_{2g}}, \eta_{e_g}$). For the nonmagnetic impurities the values for both spin directions agree. For two impurities, Cr and Mn in Cu, Table III gives a decomposition of this generalized Friedel phase shift $\eta_L(E_F)$ into the impurity phase shift $\Delta\delta_l(E_F)$ and the backscattering phase shift $\phi_L(E_F)$ [see Eq. (22)]. It is seen that the backscattering effect is quite important. Compared to Cu, the backscattering phase shifts are slightly smaller for the impurities in Ag. This is plausible since the Ag d band is about 1.7 eV lower in energy. These results are in line with earlier conclusions of Coleridge *et al.*[26] about the importance of backscattering in Cu.

Table IV gives the local charge N_{loc} in the impurity Wigner-Seitz sphere (valence electrons only). For complete screening inside the Wigner-Seitz sphere, i.e., local neutrality, this number

TABLE II. Generalized Friedel phase shifts $\eta_L(E_F)$ of 3d impurities in Cu and Ag for both spin directions.

	η_s		η_p		$\eta_{t_{2g}}$		η_{e_g}	
	↑	↓	↑	↓	↑	↓	↑	↓
*Cu*Ti[a]	−0.29		−0.21		−2.13		−2.23	
*Cu*V	−0.21	−0.25	−0.15	−0.17	−1.25	−2.29	−1.38	−2.36
*Cu*Cr	−0.15	−0.22	−0.10	−0.14	−0.46	−2.51	−0.49	−2.56
*Cu*Mn	−0.09	−0.16	−0.05	−0.10	−0.18	−2.23	−0.18	−2.31
*Cu*Fe	−0.08	−0.12	−0.04	−0.07	−0.15	−1.52	−0.15	−1.65
*Cu*Co[a]	−0.10		−0.06		−0.46		−0.49	
*Cu*Ni[a]	−0.06		−0.04		−0.20		−0.20	
*Ag*Ti	−0.11	−0.17	−0.05	−0.09	−1.63	−2.59	−1.66	−2.58
*Ag*V	−0.05	−0.17	−0.01	−0.08	−0.82	−2.79	−0.85	−2.78
*Ag*Cr	0.00	−0.15	0.03	−0.07	−0.23	−2.84	−0.24	−2.83
*Ag*Mn	0.09	−0.04	0.09	0.00	−0.03	−2.49	−0.03	−2.49
*Ag*Fe	0.07	−0.01	0.06	0.01	−0.03	−1.73	−0.03	−1.73
*Ag*Co	0.02	−0.02	0.01	−0.01	−0.08	−0.97	−0.08	−1.01
*Ag*Ni[a]	−0.01		−0.02		−0.21		−0.22	

[a] Nonmagnetic: $\eta_L^{\uparrow} = \eta_L^{\downarrow}$.

TABLE III. Impurity phase shift $\Delta\delta_l(E_F)$, backscattering phase shift $\phi_L(E_F)$, and Friedel phase shift $\eta_L(E_F) = \Delta\delta_l + \phi_L$ for Cr and Mn in Cu.

		s	p	t_{2g}	e_g
		Cr in Cu			
$\Delta\delta_l$	↑	−0.28	−0.12	−0.36	−0.36
	↓	−0.39	−0.16	−2.12	−2.12
ϕ_L	↑	0.13	0.02	−0.10	−0.13
	↓	0.18	0.03	−0.39	−0.43
η_L	↑	−0.15	−0.10	−0.46	−0.49
	↓	−0.22	−0.14	−2.51	−2.56
		Mn in Cu			
$\Delta\delta_l$	↑	−0.17	−0.06	−0.17	−0.17
	↓	−0.29	−0.12	−1.62	−1.62
ϕ_L	↑	0.08	0.01	−0.02	−0.02
	↓	0.13	0.02	−0.61	−0.69
η_L	↑	−0.09	−0.05	−0.18	−0.18
	↓	−0.16	−0.10	−2.23	−2.31

should equal to the valence Z of the impurity. It is seen that locally the impurities are rather well screened, which is another justification of our model with one perturbed muffin-tin potential only. By this we do not mean that charge-transfer effects are not important at all; however, they are rather small. Also given in Table IV are the total charges $N_{\text{tot}} = Z_0 + \Delta N(E_F)$ calculated from Lloyd's formula Eq. (22) (Z_0 equals the valence charge of the host). For an exact treatment of the screening these values have to agree with the valence Z of the impurity, since according to Friedel's sum rule $\Delta N(E_F) = Z - Z_0$. Thus the deviation from Z, e.g., the deviation of 7.08 for Mn in Ag from the correct value 7, is a measure for the accuracy of our model. In general it is seen that the Friedel sum rule is better satisfied in the middle of the $3d$ series than at both ends. Furthermore, all impurities accumulate locally more charge in Ag than in Cu. We have to concede that if these results have some physical significance we do not understand them.

Table V gives the change of $\Delta n(E_F)$ the total density of states at the Fermi energy, which can be calculated by differentiation of $\Delta N(E)$ of Eq. (22) ($\Delta n_\pm(E_F) = [d\Delta N_\pm(E)/dE]\,|_{E=E_F}$). This quantity enters, e.g., in the electronic specific heat. For each spin direction we get a maximum when the corresponding virtual bound state nearly coincides with the Fermi energy, e.g., in Cu $\Delta n_\uparrow(E_F)$ is greatest for V and $\Delta n_\downarrow(E_F)$ for Fe. Thus the sum $\Delta n(E_F) = \Delta n^+(E_F) + \Delta n^-(E_F)$ shows a double-peak structure.

Figures 4(a) and 4(b) show the residual resistivity for the $3d$ impurities in Cu and Ag. The resistivity has been calculated by the approximation proposed recently by Gupta and Benedek[31]

$$\frac{\Delta\rho}{c} = \frac{4\pi\hbar}{e^2 k_F} \sum_l (l+1) \sin^2[\eta_{l+1}(E_F) - \eta_l(E_F)] \,, \tag{29}$$

where in generalization of the impurity-in-jellium model the impurity phase shifts $\Delta\delta_l$ have been replaced by the generalized Friedel phase shifts η_l (open circles). The triangles denote experimental values. The overall agreement is reasonable.

However, there are discrepancies. Most disturbing seems to be that experimentally the minimal resistivity is found for Mn rather than for Cr. This is supported by the fact that Mn shows by far the smallest Kondo temperature which indicates that the local density of states at E_F should be smallest for Mn rather than for Cr. Note that our calculation shows that both the local density of states at E_F (Figs. 1 and 2) as well as the change of the total density of states $\Delta n(E_F)$ are smallest for Cr. On the other hand our calculations are supported by the dHvA measurements of Coleridge *et al.*[27] which seem to show that the virtual bound states of Cr, rather than Mn, are symmetrically located around the Fermi energy. Thus the situation is not clear.

D. Comparison with cluster calculations of Johnson *et al.*

Recently Johnson *et al.*[10] have performed detailed cluster calculations for magnetic impurities in Cu. The calculations are based on the self-consistent-field $X\alpha$ scattered-wave method. An impurity with 12 nearest neighbors and 6 next-nearest neighbors is considered, e.g., a $\mathrm{FeCu_{12}Cu_6}$ cluster. The re-

TABLE IV. Local valence charge N_{loc} within the impurity Wigner-Seitz sphere and total charge $N_{\text{tot}} = Z_0 + \Delta N(E_F)$ as calculated from Lloyd's formula equation (22) (Z_0 equals the valence charge of the host). For an exact treatment of the screening N_{tot} has to agree with the valence Z of the impurity [Friedel sum rule $\Delta N(E_F) = Z - Z_0$].

		Ti	V	Cr	Mn	Fe	Co	Ni
Z		4	5	6	7	8	9	10
Cu host	N_{loc}	3.53	4.66	5.74	6.79	7.90	9.02	10.04
	N_{tot}	3.75	4.78	5.88	6.87	8.06	9.33	10.23
Ag host	N_{loc}	3.73	4.85	5.91	6.90	8.02	9.12	10.18
	N_{tot}	4.06	5.09	6.03	7.08	8.26	9.32	10.28

TABLE V. Change of the total density of states $\Delta n_{\pm}(E_F)=d\Delta N_{\pm}(E)/dE\,|_{E_F}$ at the Fermi energy for up and down spin and the sum of both contributions.

		Ti	V	Cr	Mn	Fe	Co	Ni
Cu host	↑	1.24	1.97	0.53	0.10	0.10	0.88	0.26
	↓	1.24	1.05	0.67	1.42	2.97	0.88	0.26
	sum	2.47	3.02	1.20	1.52	3.07	1.75	0.51
Ag host	↑	2.67	1.80	0.28	0.04	0.05	0.13	0.55
	↓	0.74	0.35	0.27	1.38	4.74	4.44	0.55
	sum	3.41	2.15	0.55	1.41	4.79	4.57	1.11

sults of these calculations are in strong disagreement with our results. For instance, the d-wave functions $5t_{2g}$ and $5e_g$, responsible for the moment formation, are strongly delocalized (see Table I and Fig. 10 in Ref. 10); for the $5t_{2g}$ state, only 38% of the charge is localized in the Fe sphere. The spin splitting of these states (0.17 eV for e_g and 0.12 eV for t_{2g}) is an order of magnitude smaller than our spin splitting of 1.47 eV for the Fe virtual bound states. Nevertheless the moments obtained are quite high, e.g., for Mn in Cu the full atomic moment of $5\mu_B$ is obtained.

The principle defect of the cluster calculation is the neglect of the s-d interaction, i.e., the interaction with the conduction electrons of Cu. Using the golden rule (28) this interaction leads to a half-width of the virtual bound states of the order of 1 eV at the Fermi energy (see Figs. 1 and 2 and Table I). According to the Anderson model and also to our results, this interaction is decisive for the formation of local moments in metals. In order to simulate this broadening in a cluster calculation one would need many s-p states within the half-width of the virtual bound states, i.e., extremely large clusters. In the calculations of Johnson *et al.*[10] on the other hand, only one single state, the $3a_{1g}$ orbital, is "the discrete cluster analog of the half filled conduction s band of crystalline copper." Since there is no way of getting around this s-d interaction, the discrete energies of the cluster calculations should at least be broadened by the corresponding half-width. The effect of such a broadening is sketched schematically in Fig. 5. The discrete states for the spin-up and -down electrons, resembling the $5t_{2g}$ or $5e_g$ states of Johnson *et al.*, are spin-split by about 0.15 eV. For Mn the lower state is fully occupied, the higher one empty leading to a local moment of $5\mu_B$, and a Fermi energy right in the middle between these states. A Lorentzian broadening of both states by 1 eV changes the occupation drastically: The lower state is only slightly more than half filled, the higher one is slightly less than half filled, so that the local moment is practically wiped out. For the values chosen in Fig. 5 it is $0.48\mu_B$ instead of $5\mu_B$. Thus we conclude that such cluster calculations cannot give reliable results for local moments.

The importance of the interaction with the con-

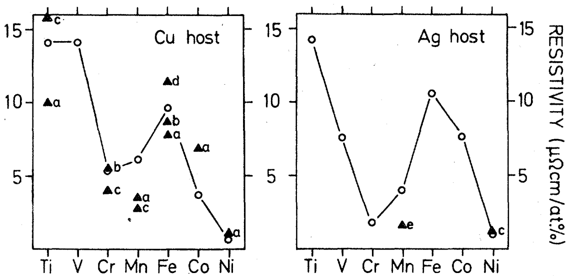

FIG. 4. Residual resistivity for impurities in Cu and Ag calculated according to Eq. (29) of Gupta and Benedek. The triangles are experimental values of different authors:

[a]G. Grüner, Adv. Phys. 23, 941 (1974).

[b]J. D. Cohen and C. P. Slichter, J. Appl. Phys. 49, 1537 (1978).

[c]J. F. Blatt, *Physics of Electronic Structure in Solids* (McGraw-Hill, New York, 1968).

[d]P. T. Coleridge *et al.*, J. Phys. F 2, 1016 (1972).

[e]Landolt-Börnstein, *Zahlenwerte und Funktionen aus Naturewissenschaften und Technik,* edited by K.-H. Hellwege (Springer, Berlin, 1979), Vol. VI, part 1.

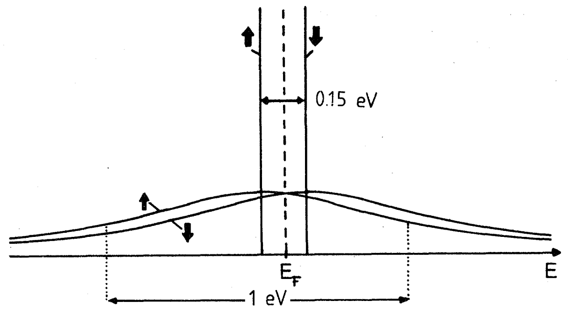

FIG. 5. Effects of broadening due to s-d interaction on the results of cluster calculations: The two discrete states with a spin splitting of 0.15 eV are broadened by a Lorentzian with a half-widths of 1 eV. Both states are now more or less equally occupied so that the moment is reduced by an order of magnitude.

duction electrons can also be seen at the case of a single impurity: Whereas a Cr or Mn atom in free space, i.e., a cluster of one atom, has only little to do with the structure of Cr or Mn impurity in Cu, the same atom embedded in jellium gives already a fair description of the impurity, as can be seen by comparing the densities of states in Fig. 2. Therefore we believe that cluster calculations as performed, e.g., by Ries and Winter,[32] where the cluster is embedded in a free electron sea, could give reliable results for magnetic impurities.

Against our approach one could argue that as a consequence of our assumption of one perturbed muffin tin the local moments have to be localized. However this is not the case, since in the Green's-function method the full spatial extent of the wave functions, densities of states, etc., is taken into account. If the displaced charge and the local moment would not be localized, it would show up in our calculation. However, our results justify our approximation as has been discussed before. This is confirmed by the recent Green's-function calculations of Baraff *et al.*[8] and Bernholc *et al.*[9] for vacancies in Si: Whereas the wave functions and the densities of states are perturbed over rather large distances away from the defect, the perturbed charge densities and the perturbed potentials are localized, since by integrating over the energy the differences in the perturbed local densities of states cancel to a large extent. Ries and Winter[33] come to the same conclusion by using their cluster method to study C vacancies in NbC.

IV. CONCLUSIONS

We have for the first time performed realistic calculations for the electronic structure of magnetic impurities in noble metals. The calculations are based on the density functional theory in the local spin-density approximation and on the KKR Green's-function method. The latter method allows a self-consistent calculation of the impurity potential. Our results for the local moments are in reasonable agreement with the available experimental information. They are in qualitative agreement with the Anderson model, although in disagreement with recent cluster calculation of Johnson *et al.*[10] in which *s*-*d* interactions are neglected.

We would like to point out that despite these successes the calculation can and will be improved in the future. In order to quantitatively discuss the question of charge transfer to nearest neighbors or the localization of the perturbed potential, changes of the potential at neighboring sites also have to be allowed. Finally, also, the problem of lattice relaxations can be attacked by these methods, as has been shown by Lodder.[34] While we believe that the main features of our present results will not be changed by such improvements, more detailed questions, e.g., whether the minimum in the density of states and in the resistivity is at Cr or at Mn, could perhaps then be answered differently.

Note added. Recently the work of Reehal and Andrews[35] and Andrews and Brown[36] on ultraviolet photoelectron spectroscopy (UPS) studies of solid solutions of $3d$ impurities in Ag and Au came to our attention. Clear evidence for the virtual bound states of Fe and Cr impurities in Au is found and especially the majority peak of Mn in $Ag_{0.8}Mn_{0.2}$ is identified at -2.8 eV below E_F which is in agreement with the findings of Norris and Wallden[22] and Wallden[23] and also with our calculations (we obtain a value of -2.4 eV; see Table I). Thus despite the negative findings of Höchst *et al.*[26] the existence of well-defined virtual bound states for magnetic impurities in noble metals seems to be now well established.

Note added in proof. Recently Cohen and Slichter[37] have fitted model calculations for $3d$ impurities in Cu to NMR satellite data for these impurities. The resulting positions of the virtual bound states are in astonishing agreement with our *ab initio* calculations.[11] This is another indication that our present calculations give a very realistic description of magnetic impurities.

APPENDIX: DYSON EQUATION FOR THE ELEMENTS $G_{LL'}^{mm'}(E)$ OF THE GREEN'S FUNCTION

According to Eq. (2) the Green's function $G(\vec{R}^m+\vec{r},\vec{R}^{m'}+\vec{r}\,')$ can be split into a Green's function $G_s^m(\vec{R}^m+\vec{r},\vec{R}^m+\vec{r}\,')$ representing the solution for a single muffin-tin potential $v_m(\vec{r})$ and into a second term containing only regular radial functions $R_l^m(r,E)$ and $R_{l'}^{m'}(r',E)$:

$$G(\vec{R}^m+\vec{r},\vec{R}^{m'}+\vec{r}\,')=\delta_{mm'}G_s^m(\vec{R}^m+\vec{r},\vec{R}^m+\vec{r}\,')+\sum_{LL'}R_l^m(r,E)Y_L(\vec{r})G_{LL'}^{mm'}(E)R_{l'}^{m'}(r',E)Y_{L'}(\vec{r}\,') \tag{A1}$$

with

$$G_s^m(\vec{R}^m+\vec{r},\vec{R}^m+\vec{r}\,')=\frac{2m}{\hbar^2}K\sum_L R_l^m(r_<,E)Y_L(\vec{r})H_l^m(r_>,E)Y_L(\vec{r}\,')\,. \tag{A2}$$

The same equations hold for the Green's functions G^0 for the ideal crystal if the radial wave functions are replaced by $R_l^0(r,E), H_l^0(r,E)$. The corresponding elements of the Green's function are $G_{LL'}^{0\,(m-m')}(E)$.

By inserting these expressions into the Lippmann-Schwinger equation (5), the terms proportional to $\delta_{mm'}$ can be collected and represent a Lippmann-Schwinger equation for $G_s^m(\vec{R}^m+\vec{r},\vec{R}^m+\vec{r}\,')$:

$$G_s^m(\vec{R}^m+\vec{r},\vec{R}^m+\vec{r}\,')=G_s^0(\vec{R}^m+\vec{r},\vec{R}^m+\vec{r}\,')+\int d\vec{r}\,''G_s^0(\vec{R}^m+\vec{r},\vec{R}^m+\vec{r}\,'')\Delta v_m(\vec{r}\,'')G_s^m(\vec{R}^m+\vec{r}\,'',\vec{R}^m+\vec{r}\,')\,. \tag{A3}$$

The remaining terms lead to the following equation for $G_{LL'}^{mm'}$ in terms of $G_{LL'}^{0\,mm'}$:

$$\begin{aligned}R_l^m(r)G_{LL'}^{mm'}R_{l'}^{m'}(r')={}&R_l^0(r)G_{LL'}^{0\,mm'}R_{l'}^0(r')+\frac{2m}{\hbar^2}K\int_0^{R_{\mathrm{MT}}}dr''r''^2R_l^0(r_<'')H_l^0(r_>'')\Delta v_m(r'')R_l^m(r'')G_{LL'}^{mm'}R_{l'}^{m'}(r')\\&+\frac{2m}{\hbar^2}KR_l^0(r)G_{LL'}^{0\,mm'}\int_0^{R_{\mathrm{MT}}}r''^2dr''R_{l'}^0(r'')\Delta v_m(r'')R_l^m(r_<'')H_l^m(r_>'')\\&+R_l^0(r)\sum_{nL''}G_{LL''}^{0\,mn}\int_0^{R_{\mathrm{MT}}}r''^2dr''R_l^0(r'')\Delta v_n(r'')R_{l''}^n(r'')G_{L''L'}^{nm'}R_{l'}^{m'}(r')\,.\end{aligned} \tag{A4}$$

Note that in the second term $r_<''$ means the minimum of r,r'', however, in the third term $r_<''$ stands for the minimum of r' and r''. By realizing that the radial solutions $\tilde{R}_l^m(r,E)=e^{i\delta_l^m(E)}R_l^m(r,E)$ satisfy the radial Schrödinger equation

$$\tilde{R}_l^m(r,E)=\tilde{R}_l^0(r,E)+\int_0^{R_{\mathrm{MT}}}r''^2dr''\,\frac{2m}{\hbar^2}KR_l^0(r_<''E)H_l^0(r_>''E)\Delta v_m(r'')\tilde{R}_l^m(r'',E)\,, \tag{A5}$$

with $\tilde{R}_l^0(r)=e^{i\delta_l^0}R_l^0(r)$, the second term on the right-hand side of Eq. (A4) can be lumped together with the left-hand side of Eq. (A4) thus replacing $R_l^m(r)$ by $e^{-i\delta_l^m+i\delta_l^0}R_l^0(r)$. Analogously the first and third terms on the right-hand side of Eq. (A4) can be lumped together, effectively replacing $R_{l'}^0(r')$ in the first term by $e^{-i\delta_{l'}^0+i\delta_{l'}^{m'}}R_{l'}^{m'}(r')$. For the latter step we have used the following version of the Lippmann-Schwinger equation:

$$\tilde{R}_l^m(r,E)=\tilde{R}_l^0(r,E)+\int_0^{R_{\mathrm{MT}}}r''^2dr''\,\frac{2m}{\hbar^2}KR_l^m(r_<'',E)H_l^m(r_>'',E)\Delta v_m(r'')\tilde{R}^0(r'',E)\,. \tag{A6}$$

The resulting equation then takes the form

$$\begin{aligned}R_l^0(r)e^{-i\delta_l^m+i\delta_l^0}G_{LL'}^{mm'}R_{l'}^{m'}(r')={}&R_l^0(r)G_{LL'}^{0\,mm'}e^{-i\delta_{l'}^0+i\delta_{l'}^{m'}}R_{l'}^{m'}(r')\\&+R_l^0(r)\sum_{nL''}G_{LL''}^{0\,mn}\left(\int_0^{R_{\mathrm{MT}}}r''^2dr''R_{l''}^0(r'')\Delta v_n(r'')R_{l''}^n(r'')\right)G_{L''L'}^{nm'}R_{l'}^{m'}(r')\,.\end{aligned} \tag{A7}$$

Since all three terms contain the same radial functions, we obtain the desired equation for $G_{LL'}^{mm'}$ in terms of $G_{LL'}^{0\,mm'}$:

$$\tilde{G}_{LL'}^{mm'}=\tilde{G}_{LL'}^{0\,(m-m')}+\sum_{nL''}\tilde{G}_{LL''}^{0\,(m-n)}\Delta t_{L''}^n\tilde{G}_{L''L'}^{nm'}\,, \tag{A8}$$

with

$$\tilde{G}_{LL'}^{mm'}=e^{-i\delta_l^m}G_{LL'}^{mm'}e^{-i\delta_{L'}^{m'}}\,,$$

$$\tilde{G}_{LL'}^{0\,(m-m')}=e^{-i\delta_l^0}G_{LL'}^{0\,(m-m')}e^{-i\delta_{l'}^0}\,.$$

In these equations the deviations of the on-shell t matrices $t_l^m(E)$ from the ideal crystal values $t_l^0(E)$ appear as perturbing potentials.

$$\Delta t_l^m(E)=\int_0^\infty r''^2dr''\tilde{R}_l^0(r'',E)\Delta v_m(r'')\tilde{R}_{l''}^m(r'',E) \tag{A9}$$

or

$$\Delta t_l^m(E)=-\frac{e^{i(\delta_l^m+\delta_l^0)}}{K}\sin(\delta_l^m-\delta_l^0)\,\frac{\hbar^2}{2m}=t_l^m(E)-t_l^0(E) \tag{A10}$$

with

$$t_l^m(E)=-\frac{e^{i\delta_l^m}}{K}(\sin\delta_l^m)\,\frac{\hbar^2}{2m}\,.$$

The expressions (A9) and (A10) are equivalent which is seen as follows: In the integral (A9) we can replace the terms $v_m(r)\tilde{R}_l^m(r)$ and $v^0(r)\tilde{R}_l^0(r)$ by the following expressions obtained from the radial Schrödinger equation:

$$v_m(r)\tilde{R}_l^m(r)=\left(E-\frac{\hbar^2}{2m}\frac{l(l+1)}{r^2}+\frac{\hbar^2}{2m}\frac{1}{r}\,\partial_r^2r\right)\tilde{R}_l^m(r)\,, \tag{A11}$$

$$v^0(r)\tilde{R}_l^0(r)=\left(E-\frac{\hbar^2}{2m}\frac{l(l+1)}{r^2}+\frac{\hbar^2}{2m}\frac{1}{r}\,\partial_r^2r\right)\tilde{R}_l^0(r)\,. \tag{A12}$$

Only the terms containing the second derivative of $r\tilde{R}_l^m$ and $r\tilde{R}_l^0$ remain. The resulting integrand is

$$\frac{d}{dr}\left(r^2\tilde{R}_l^0(r)\,\frac{d\tilde{R}_l^m(r)}{dr}-r^2\,\frac{d\tilde{R}_l^0(r)}{dr}\,\tilde{R}_l^m(r)\right)\,, \tag{A13}$$

so that the integral is elementary and given by the value of the radial functions and their first derivatives at the muffin-tin radius. We have

$$\Delta t_l^m(E)=\left(r^2\tilde{R}_l^0(r)\frac{d\tilde{R}_l^m}{dr}-r^2\frac{d\tilde{R}_l^0(r)}{dr}\,\tilde{R}_l^m(r)\right)\Bigg|_{r=R_{\mathrm{MT}}}. \tag{A14}$$

This expression can readily be calculated using the asymptotic result (4) for the wave functions and the Wronskian for $j_l(x)$ and $n_l(x)$:

$$j_l(x)n_l'(x)-j_l'(x)n_l(x)=+1/x^2\,, \tag{A15}$$

which finally leads to the result (A10).

Very analogous to the relation (8) between the Green's function $G_{LL'}^{mm'}$ and the ideal crystal Green's function we can also derive the corresponding Eq. (7) between $G_{LL'}^{mm'}$ and the free-space Green's function $g_{LL'}^{mm'}$. Inserting the equation for g

$$g(\vec{\mathrm{R}}^m+\vec{\mathrm{r}},\vec{\mathrm{R}}^{m'}+\vec{\mathrm{r}}\,')=\delta_{mm'}\frac{2m}{\hbar^2}K\sum_L j_l(Kr_<)Y_L(\vec{\mathrm{r}})h_l(Kr_>)Y_L(\vec{\mathrm{r}}\,')+\sum_{LL'}j_l(Kr)Y_L(\vec{\mathrm{r}})g_{LL'}^{mm'}j_{l'}(Kr')Y_{L'}(\vec{\mathrm{r}}\,')\,,$$

together with (A1) into Eq. (5), the terms proportional to $\delta_{mm'}$ give an equation analogous to (A5) for G_s^m, where $G_s^0(\vec{\mathrm{R}}^m+\vec{\mathrm{r}},\vec{\mathrm{R}}^m+\vec{\mathrm{r}}\,')$ is replaced by $g(\vec{\mathrm{R}}^m+\vec{\mathrm{r}},\vec{\mathrm{R}}^m+\vec{\mathrm{r}}\,')$ and $\Delta v_m(r'')$ by $v_m(r'')$. The remaining equation analogous to (A4) can be modified using similar arguments as in (A5) and (A6) and finally leads to the desired equation between $G_{LL'}^{mm'}$ and $g_{LL'}^{mm'}$

$$\tilde{G}_{LL'}^{mm'}=g_{LL'}^{(m-m')}+\sum_{nL''}g_{LL''}^{(m-n)}t_{l''}^n\tilde{G}_{L''L'}^{nm'}\,.$$

The t matrix $t_l^m(E)$ is obtained as

$$\begin{aligned}t_l^m(E)&=\int_0^{R_{\mathrm{MT}}}r''^2dr''j_l(Kr'')v_m(r'')\tilde{R}_l^m(r'')\\&=-\frac{\hbar^2}{2m}\frac{e^{i\delta_l^m}}{K}\sin\delta_l^m\,,\end{aligned}$$

where the last identity follows using relations similar to Eqs. (A11)–(A15).

---

*Present address: Institut für Physikalische Chemie, Universität Wien, Währingerstrasse 42, A1090 Wien, Austria.

[1] P. W. Anderson, Phys. Rev. 124, 41 (1961).

[2] P. A. Wolff, Phys. Rev. 124, 1030 (1961).

[3] J. R. Schrieffer, J. Appl. Phys. 38, 1143 (1967).

[4] L. L. Hirst, Phys. Kondens. Mater. 11, 255 (1970); Z. Phys. 241, 9 (1971).

[5] See, e.g., V. L. Moruzzi, A. R. Williams, and J. F. Janak, Phys. Rev. B 15, 2854 (1977); D. E. Eastman, F. J. Himpsel, and J. A. Knapp, Phys. Rev. Lett. 44, 95 (1980); U. K. Poulsen, J. Kollár, and O. K. Andersen, J. Phys. F 6, L241 (1976); Physica (Utrecht) 86–88 B, 249 (1977).

[6] T. H. Dupree, Ann. Phys. (N. Y.) 15, 63 (1961).

[7] J. L. Beeby, Proc. R. Soc. London Ser. A 302, 113 (1967).

[8] G. A. Baraff and M. Schlüter, Phys. Rev. Lett. 41, 892 (1978).

[9] J. Bernholc, N. O. Lipari, and S. T. Pantelides, Phys. Rev. Lett. 41, 895 (1978).

[10] K. H. Johnson, D. D. Vredensky, and R. P. Messmer, Phys. Rev. B 19, 1519 (1979).

[11] R. Zeller, R. Podloucky, and P. H. Dederichs, Z. Phys. B 38, 165 (1980).

[12] J. Morgan, Proc. R. Soc. London 16, 365 (1966).

[13] N. A. W. Holzwarth, Phys. Rev. B 11, 3718 (1975).

[14] G. Lehmann, Phys. Status Solidi B 70, 735 (1975).

[15] R. Harris, J. Phys. C 3, 172 (1970).

[16] M. Hamasaki, S. Asano, and J. Yamashita, J. Phys. Soc. Jpn. 41, 378 (1976).

[17] R. Zeller and P. H. Dederichs, Phys. Rev. Lett. 42, 1713 (1979).

[18] P. Lloyd, Proc. Phys. Soc. London 90, 207 (1967).

[19] U. von Barth and L. Hedin, J. Phys. C 5, 1629 (1972).

[20] V. L. Moruzzi, J. F. Janak, and A. R. Williams, *Calculated Electronic Properties of Metals* (Pergamon, New York, 1978).

[21] J. D. Cohen and C. P. Slichter, J. Appl. Phys. 49, 1537 (1978).

[22] C. Norris, L. Walldén, Solid State Commun. 7, 99 (1969).

[23] L. Wallden, Philos. Mag. 21, 571 (1970).

[24] H. P. Myers, L. Walldén, and A. Karlsson, Philos. Mag. 18, 725 (1968).

[25] M. R. Steel and D. M. Treherne, J. Phys. F 2, 199 (1972).

[26] H. Höchst, P. Steiner, and S. Hüfner, Z. Phys. B 38, 201 (1980).

[27] P. T. Coleridge, G. B. Scott, and I. M. Templeton, Can. J. Phys. 50, 1999 (1972).

[28] D. Sang and A. Myers, J. Phys. F 6, 545 (1976).

[29] M. Labro, private communication.

[30] O. Gunnarsson, J. Phys. F 6, 587 (1976).

[31] R. P. Gupta and R. Benedek, Phys. Rev. B 19, 583 (1979).

[32] G. Ries and H. Winter, J. Phys. F 9, 1589 (1979).

[33] G. Ries and H. Winter, J. Phys. F (in press).

[34] A. Lodder, J. Phys. F 6, 1885 (1976); 7, 139 (1977).

[35] H. S. Reehal and P. T. Andrews, J. Phys. F 10, 1631 (1980).

[36] P. T. Andrews and L. T. Brown, in Proceedings of the Conference on Physics of Transition Metals, Leeds, 1980 (in press).

[37] J. D. Cohen and C. P. Slichter, Phys. Rev. B 22, 45 (1980).